Assay of Biothiols by Regulating the Growth of Silver Nanoparticles with C-Dots as Reducing Agent

ARTICLE *in* ANALYTICAL CHEMISTRY · APRIL 2014

Impact Factor: 5.64 · DOI: 10.1021/ac500601k · Source: PubMed

5 AUTHORS, INCLUDING:

Xu-Wei Chen
Northeastern University (Shenyang, China)
79 PUBLICATIONS **1,720** CITATIONS

SEE PROFILE

analytical chemistry

Article

pubs.acs.org/ac

Assay of Biothiols by Regulating the Growth of Silver Nanoparticles with C-Dots as Reducing Agent

Li-Ming Shen,[†] Qing Chen,[†] Zheng-Yue Sun,[†] Xu-Wei Chen,*[,†] and Jian-Hua Wang*[,†,‡]

[†]Research Center for Analytical Sciences, College of Sciences, Northeastern University, Box 332, Shenyang, Liaoning 110819, China

[‡]Collaborative Innovation Center of Chemical Science and Engineering, Tianjin 300071, China

Supporting Information

ABSTRACT: Recently, the development of optical probes for the assay of thiols, e.g., cysteine (Cys), homocysteine (Hcy), and glutathione (GSH), has been an active research area due to their biological significance. We have found that carbon dots (C-dots) exhibit direct reduction of Ag^+ to elemental silver (Ag^0) and the resulting Ag^0 formed a silver nanoparticle (Ag-NP) spontaneously. The excessive C-dots consume free Ag^+ in the solution by binding Ag^+ with functional groups on the C-dots surface and thus inhibits the growth of Ag-NPs. Biothiols can coordinate with Ag^+ through thiol groups, and afterward, the Ag^+-biothiol complex gradually releases free Ag^+ to ensure its reduction by C-dots and thus facilitates the growth of Ag-NPs on C-dots surface. A colorimetric assay procedure is thus developed for fast detection of biothiols based on Ag-NPs plasmon absorption. The linear calibration range can be regulated by controlling the concentration of Ag^+. Two linear ranges were obtained for the biothiols assay at different levels, which offer ultrahigh sensitivity for the assay of an ultratrace amount of biothiols with detection limits of 1.5, 2.6, and 1.2 nM for Cys, Hcy, and GSH, respectively. The precisions for the assay of Cys, Hcy, and GSH at 20 nM are achieved as 3.1%, 3.1%, and 2.4%. In addition, the sensing system exhibits good selectivity toward biothiols in the presence of other amino acids, the major metal cations, and biomolecules in biological fluids. For the assay of 20 nM Cys, 150-fold of coexisting amino acids, 2500-fold of Ca^{2+}, Mg^{2+}, glucose, and ascorbic acid, and 38-fold of HSA are tolerated. In the assay of Cys in human plasma, spiking recoveries of 94% to 108% are obtained at 100 μM.

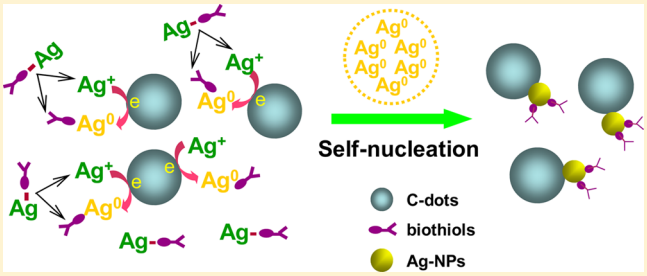

Biothiols, such as cysteine (Cys), homocysteine (Hcy), and glutathione (GSH), are components of many proteins and molecules in biological systems and play pivotal roles in the cellular antioxidant defense system for their participation in the process of reversible redox reactions.[1,2] The alternation of thiols concentration in the human body has been linked to a number of diseases. Specifically, Cys deficiency results in a series of disorders in living systems, e.g., slowing down the growth in children and depigmentation of hair; it also causes edema, lethargy, liver damage, and loss of muscle and fat as well as skin lesions.[3] While an elevated level of Cys is associated with neurotoxicity,[4] on the other hand, an elevated plasma Hcy level is a strong, independent risk factor for the development of dementia and Alzheimer's disease. It also seems to be a particularly strong predictor of cardiovascular mortality.[5,6] As the most abundant nonprotein thiol, GSH plays multifunctions within cells, detoxification of free radicals and peroxides, regulation of cell growth and protein function, and maintenance of immune function.[7] Individuals infected with human immunodeficiency virus (HIV) have a decrease of GSH in plasma which may potentiate HIV replication and accelerate disease progression. Moreover, GSH deficiency contributes to overall depression of immune functions.[8] Because of these important biological functions of thiols, considerable attention has been drawn to their highly sensitive and selective assay in biological systems. Among those reported procedures, optical assay approaches based on colorimetry and fluorescence have apparent advantages over other methods in terms of sensitivity and ease of operation.[9−18]

By exploiting the strong affinity of biothiols toward metal cations and metal nanoparticles, a variety of optosensors were constructed with high sensitivity and selectivity.[19,20] Ag^+ and Hg^{2+} can selectively bind to a few native or artificial bases in DNA duplexes to form metal-mediated base pairs, yet the presence of biothiols will disturb the coordination between metal cations and DNA because Ag^+ and Hg^{2+} is apt to interact with thiols. In combination with optical probes, this competition mechanism can be applied to the assay of thiols.[21−24] On the other hand, biothiols-induced aggregation of Au nanorods and nanoparticles results in a decrease in the surface plasmon resonance absorption at short wavelength and meanwhile gives rise to an absorption band at a longer wavelength. This made the assay of biothiols possible.[25−28]

Recently, carbon nanodots (C-dots) have drawn extensive attention in various fields owing to their stable physicochemical and photochemical properties.[29] The well-defined and ultrafine

Received: February 12, 2014
Accepted: April 28, 2014
Published: April 28, 2014

   dx.doi.org/10.1021/ac500601k | *Anal. Chem.* 2014, 86, 5002−5008

dimensions of C-dots, in addition to the development of simple preparation approaches,[30−34] provide an encouraging platform for imaging and sensing,[35,36] medical diagnosis,[37] and catalysis and photovoltaic devices.[38,39] Most notably, C-dots offer an alternative to organic dyes and semiconductor quantum dots in optical biosensing and bioimaging due to their tunable surface functionalities, excellent photostability, and favorable biocompatibility.[36,40−46] Up to now, most biosensors of this type are developed on the basis of fluorescence quenching of C-dots triggered by analytes,[43−46] and these "turn-off" optical sensors are vulnerable to interferences. Therefore, further studies are urgently necessary to explore the full potential of C-dots for developing advanced smart sensors.

It is known that C-dots are both excellent electron acceptors and electron donors, which have promising potentials as an oxidizing or reducing agent.[47−51] We have successfully fabricated stable silver nanoparticles (Ag-NPs) with C-dots acting as a catalytic reductant and capping agent.[52] The abundant reductive groups on the surface of C-dots, such as hydroxyl moieties, endow C-dots function as nucleation centers for the nucleation and growth of metallic nanoparticles and act as a stabilizer to prevent aggregation of nanoparticles derived from metal salts. In the present work, we found that excessive C-dots inhibit the growth of Ag-NPs due to the lack of free Ag^+ in solution, while the presence of biothiols stimulates the production of Ag-NPs. Biothiols bind Ag^+ through thiol groups, and the formed Ag^+-biothiol complex gradually releases free Ag^+ to be reduced by C-dots on their surface and facilitates in situ growth of silver nanoparticles. The optical properties of the generated metallic particles enable the quantitative assay of biothiols in the nanomolar range with favorable selectivity. The fast detection of biothiols is realized by fabrication of an ultrasensitive and label-free colorimetric method. Validation of the proposed assay procedure with human plasma samples demonstrated a potential for the diagnosis of related diseases.

EXPERIMENTAL SECTION

Apparatus and Chemicals. UV−vis absorption spectra were recorded with a U-3900 UV−vis spectrophotometer (Hitachi, Japan) with a 1.0 cm quartz cell. Transmission electron microscopy (TEM) images were recorded on a field-emission transmission electron microscope at an accelerating voltage of 200 kV (JEM-2100F, JEOL, Ltd., Japan). FT-IR spectra were obtained by using a Nicolet-6700 FT-IR spectrometer (Thermo Ltd., USA) within a range of 4000−500 cm^{-1}. Circular dichroism spectra were recorded on a MOS-450 spectrometer/polarimeter (Biologic Science Instrument, France) and are acquired every 1 nm with a bandwidth setting of 1 nm under nitrogen protection. The other equipment used include an IKA vortex 3 (IKA Ltd., Germany), a GZX 9030 MBE electrothermal blowing drybox (Shanghai Boxun Ltd., China), and a freezing drier (Beijing Boyikang Ltd., China).

$AgNO_3$, $Ca(NO_3)_2$, $Mg(NO_3)_2$, NaOH, and *N*-ethylmaleimide (NEM) were obtained from Sinopharm Chemical Reagent Co. (Shanghai, China). L-Cysteine (Cys), glutamine (Gln), asparagine (Asn), alanine (Ala), arginine (Arg), aspartic acid (Asp), glutamic acid (Glu), glycine (Gly), histidine (His), isoleucine (Ile), leucine (Leu), lysine (Lys), methionine (Met), phenylalanine (Phe), serine (Ser), threonine (Thr), tyrosine (Tyr), valine (Val), proline (Pro), and tryptophan (Trp) were obtained from Beijing Biotopped Science & Technology Co., Ltd. (Beijing, China) and used without further purification. Ascorbic acid (AA) and glucose anhydrouse (glu) were acquired from Tianjin Damao Chemical Regeant Factory (Tianjin, China). Homocysteine (Hcy), reduced glutathione (GSH), and human serum albumin (HSA) were purchased from Sigma-Aldrich (St. Louis, USA). Deionized (DI) water of 18 MΩ cm was used throughout the experiments.

Preparation of C-Dots. C-dots were fabricated by hydrothermal carbonization of chitosan at a mild temperature according to a published procedure with slight modification.[53] C-dots derived from chitosan are prepared by heating 4 g of chitosan in 36 mL of 2% acetic acid in a 100 mL Teflon equipped stainless steel autoclave at 180 °C for 12 h. After cooling to room temperature, the obtained dark brown product is centrifuged at a high speed (12 000 rpm) for 25 min to remove the less-fluorescent deposit. The upper brown solution is then filtered with a 0.22 μm filter membrane for purification. The C-dots stock solution was stored in a refrigerator at 4 °C for future use.

The Growth of Silver Nanoparticles with C-Dots as Reducing Agent. We have demonstrated that C-dots can reduce Ag^+ to elemental Ag^0 and create AgNPs simultaneously. In the meantime, C-dots act as capping agents to protect the AgNPs from agglomeration. When there are excessive C-dots, the growth of Ag-NPs is significantly suppressed. The addition of biothiols regulates the growth of Ag-NPs by combining Ag^+ with thiol groups and facilitating the synthesis of metallic nanoparticles. Moreover, the increase of the quantity of Ag-NPs correlates closely with the concentration of biothiols and thus entails quantitative detection of biothiols in aqueous medium.

In the practical assay, the stock solutions of $AgNO_3$ and biothiols were freshly prepared. To a 2 mL calibrated test tube, C-dots (0.23 or 0.21 g L^{-1}), H_2O, a certain amount of analytes (biothiols, 20−400 nM and 2.5−30 nM), Ag^+ (0.2 mM or 0.1 mM), and NaOH (0.01 or 0.05 M) were sequentially added and the mixture was thoroughly mixed. The test tube was then put into a 50 or 70 °C water bath for incubating for 5 min. After cooling to room temperature, the UV−vis spectra are recorded.

Measurement of Circular Dichroism (CD) Spectra. As the CD spectrum of the Ag^+-Cys complex is pH sensitive,[54] the measurement of CD spectra in the present study is conducted in aqueous medium without NaOH. The CD spectra of Cys (0.5 mM), Ag^+ (0.5 mM), C-dots (0.52 g L^{-1}), and Ag^+-Cys complex (0.5 mM) were recorded as control. The measurement was performed immediately upon mixing of Cys (0.5 mM), C-dots (0.52 g L^{-1}), and Ag^+ (0.5 mM). Afterward, the mixture of Cys, C-dots, and Ag^+ was incubated in a 70 °C water bath for 20 min and then cooled down to room temperature, followed by measurement of CD spectra.

Biothiols Sensing in Biological Fluids. Human serum samples were provided by the Sheng-Jing Hospital of China Medical University (Shenyang, China). A 100-fold dilution of the plasma was adopted for the measurement. Twenty μL was mixed with C-dots (0.21 g L^{-1}), NaOH (0.05 M), and Ag^+ (0.1 mM) for incubation at 70 °C for 5 min, and another 20 μL was pretreated with 0.05 mM NEM as a thiol-blocking compound before reaction with C-dots. Finally, UV−vis spectra at a wavelength of 430 nm were recorded.

RESULTS AND DISCUSSION

Effect of C-Dots and Cysteine on the Growth of Silver Nanoparticles. We found an interesting phenomenon during the growth of Ag nanoparticles with C-dots as reducing agent and stabilizer. That is, the amount of Ag nanoparticles

dx.doi.org/10.1021/ac500601k | Anal. Chem. 2014, 86, 5002−5008

decreased with the increase of the C-dots concentration (Figure 1A). However, when thiols, e.g., cysteine, were introduced, the

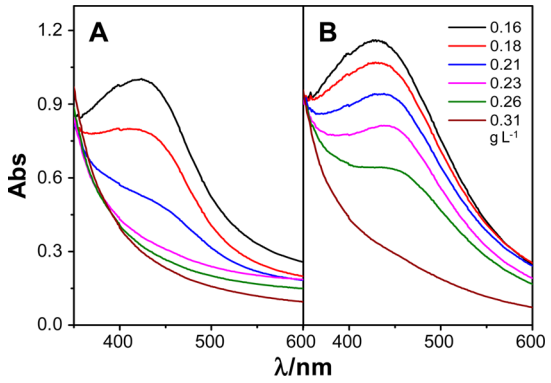

Figure 1. UV−vis spectra of the nanocomposite after incubating $AgNO_3$ (0.2 mM) with C-dots (0.16−0.31 g L^{-1}) in the absence (A) and presence (B) of cysteine (100 nM) in 0.01 M NaOH at 50 °C for 5 min.

growth of silver nanoparticles was obviously stimulated (Figure 1B). According to the mechanisms proposed by LaMer and co-workers, the building blocks of a metal nanocrystal, e.g., Ag(0) in the present case, steadily increase with time as the precursor is decomposed. Once the concentration of atoms reaches a point of supersaturation, the atoms start to aggregate into small clusters (i.e., nuclei) via self (or homogeneous) nucleation. With a continuous supply of atoms via ongoing precursor decomposition, the nuclei will grow into nanocrystals of increasingly larger size.[55,56] In the present system, the growth of NPs was initiated from the C-dots surface, and the first step was the binding of silver ions to the reductive groups on the surface of C-dots (amine and phenol hydroxyl). For the growth of stable and small-sized Ag-NPs (3.1 ± 1.5 nm), the concentration of C-dots is 0.033 g L^{-1}.[52] In our case, an excessive amount of C-dots, i.e., 0.23 g L^{-1}, is used. The majority of Ag^+ was adsorbed onto the surface of C-dots, and the number of free Ag^+ in solution is decreased significantly. The reduced Ag (0) adhered onto the C-dots surface excluded their aggregation into small clusters. In addition, there is no continuous supply of free Ag^+ from the solution to be reduced to Ag(0); thus, the nucleation and growth of nanocrystals was partially blocked and, consequently, resulted in the decrease of the number of silver nanoparticles.

Cysteine is a kind of reducing agent. It was reported that the exposure of Ag^+-Cys complexes to UV irradiation at λ 254 nm for 15 min resulted in the formation of AgNPs,[57] However, cysteine itself cannot induce the growth of Ag-NPs after incubation with $AgNO_3$ in the present system. When increasing the concentration of cysteine, no Ag-NPs surface plasmon resonance (SPR) was identified in the UV−vis spectra (as shown in Supporting Information Figure S1). In order to investigate the role of cysteine during the production of Ag-NPs, circular dichroism (CD) spectra are recorded as illustrated in Figure 2. Two unique CD peaks at 267 and 300 nm were found for C-dots. Upon mixing C-dots with Ag^+ and cysteine, the formation of Ag^+-Cys complex was identified by the appearance of two significant CD peaks at 248 and 363 nm, the same as those reported for the Ag^+-Cys complex.[54,57,58] It can be seen that the peaks at 232, 283, and 314 nm were shifted to longer wavelength compared to Ag^+-Cys complex. The CD spectrum of the mixture of C-dots, Ag^+, and cysteine is the

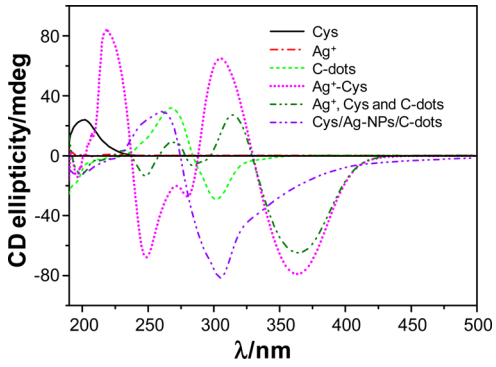

Figure 2. CD spectra of cysteine (0.5 mM); Ag^+ (0.5 mM); C-dots (0.52 g L^{-1}); Ag^+-Cys complex (0.5 mM); mixture of cysteine (0.5 mM), C-dots (0.52 g L^{-1}) and Ag^+ (0.5 mM); and Cys/Ag-NPs/C-dots.

combination of C-dots and Ag^+-Cys complex and also shows the characteristic CD peak of C-dots at 268 nm. After incubating the mixture in a 70 °C water bath for 20 min, a color change from clear to vibrant deep yellow was observed indicating the formation of Ag-NPs. Meanwhile, characteristic CD peaks of the Ag^+-Cys complex have disappeared and the final product, i.e., the Cys/Ag-NPs/C-dots composite, exhibited only the characteristic CD peaks of C-dots. The above observations demonstrated the complexation of Ag^+ with cysteine to form a complex instantaneously upon mixing. Considering that cysteine itself is unable to induce the conversion of Ag^+ to Ag^0 and the reducing capability of C-dots is stronger than that of cysteine, the Ag^+-Cys complex gradually release Ag^+ to ensure the supply of free Ag^+ to the surface of C-dots and facilitate the formation of more Ag-NPs. It is also assumed that cysteine acts as a stabilizing agent for the Ag-NPs/C-dots composite.[59] It is found that the Ag-NPs/C-dots composite is not stable in the presence of only C-dots, while Cys/Ag-NPs/C-dots can be stable for a longer time (2 days).

FT-IR spectra further demonstrated the role of cysteine acting as a capping agent. It was found that the stretching vibration band of S−H of free cysteine at 2555 cm^{-1} disappeared in the Cys/Ag-NPs/C-dots composite owing to the binding of thiol group to Ag-NPs (Figure 3).[57] Meanwhile, the 3430 cm^{-1} stretching vibration band of −OH and $-NH_2$ for C-dots shifted to 3310 cm^{-1} which is attributed to the comprehensive effect of the −OH group (carboxylic acid) in

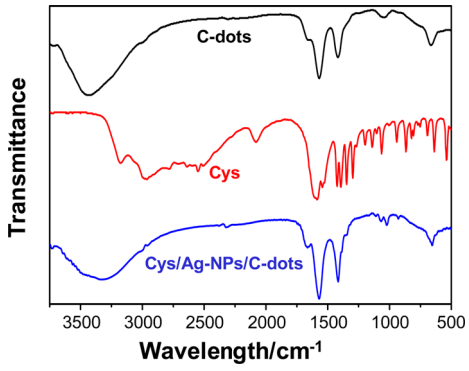

Figure 3. FT-IR spectra of C-dots, Cys, and Cys/Ag-NPs/C-dots composite.

dx.doi.org/10.1021/ac500601k | Anal. Chem. 2014, 86, 5002−5008

cysteine. The investigations of CD and FT-IR spectra allowed us to suggest that cysteine can simultaneously act as complexing and protecting agents to promote the growth of Ag-NPs.

TEM images showed that the average size of the Ag-NPs prepared from the surface of C-dots is 17.4 ± 5.7 nm, and the nanoparticles are uniformly distributed as illustrated in Figure 4A. However, in the presence of C-dots and cysteine, the size

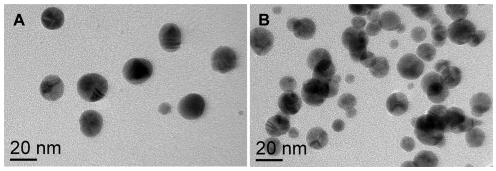

Figure 4. (A) HRTEM images of the Ag-NPs/C-dots composites made from $AgNO_3$ (0.2 mM) and C-dots (0.23 g L^{-1}) in 0.01 M NaOH incubating at 50 °C for 5 min; (B) HRTEM images of the Cys/Ag-NPs/C-dots composites made from $AgNO_3$ (0.2 mM), Cys (100 nM), and C-dots (0.23 g L^{-1}) in 0.01 M NaOH incubating at 50 °C for 5 min.

distribution of 13.8 ± 4.2 nm for the prepared Ag-NPs exhibits a wider range with some smaller sized nanoparticles (Figure 4B). This observation indicated that cysteine functioning as capping agent will modulate the size of the Ag-NPs and can be the cause of their inhomogeneous size distribution.[60]

Increase of Absorbance Induced by Cysteine. For the purpose of quantitative analysis, it is desired to maximize the difference between the absorbance in the absence and in the presence of cysteine. For this purpose, we have thoroughly examined the major factors affecting the growth of Ag-NPs, i.e., the concentration of C-dots and Ag^+, in the presence of 100 nM cysteine. It is seen from Figure 1A that, with the increase of C-dots concentration, the absorbance of Ag-NPs at 430 nm decreased significantly. As the C-dots concentration exceeds 0.23 g L^{-1}, there is completely no characteristic absorbance at around 400 nm. Figure 1B illustrated an increase in the absorbance with the addition of cysteine, attributed to the formation of Ag-NPs through progressive release of free Ag^+ from the Ag^+-Cys complex and their reduction by C-dots. Figure 5A indicated the variation of net absorbance increase of Ag-NPs stimulated by 100 nM cysteine, and a maximum absorbance increase was obtained at a C-dots concentration of 0.23 g L^{-1}. Panels A and B in Supporting Information Figure S2 showed the dependence of absorbance characteristic to the plasmon of Ag-NPs on the concentration of Ag^+. Notably, when the concentration of Ag^+ increased from 0.06 to 0.20 mM, UV−vis spectra did not show any obvious difference in the absence of cysteine, while the spectra are intensified significantly both with and without cysteine as the concentration of Ag^+ is above 0.2 mM (Figure 5B). This is because of the large amount of C-dots in the system; Ag^+ ranging from 0.06 to 0.20 mM was completely bound onto the surface of C-dots, and there is no free Ag^+ in the solution, so that the growth of Ag-NPs is suppressed. By adding more Ag^+ into the solution, the amount of free Ag^+ increases and thus more Ag-NPs can be formed as discussed previously. For convenience, cysteine was incubated together with C-dots and Ag^+, in which cysteine binds with Ag^+ first and then gradually releases free Ag^+ to ensure the formation of Ag-NPs, which in turn gives rise to a significant increase in the absorbance.

Quantitative Assay of Biothiols by Silver Nanoparticle-Induced Plasmon. UV−vis spectra in the presence of various concentrations of cysteine with 0.2 mM Ag^+ are shown in Figure 6A. The increase of cysteine concentration results in a slight blue shift of the absorbance maximum. The smaller size of Ag-NPs observed in the TEM image as illustrated in Figure 4B explains this blue-shift. A linear relationship between the net absorbance increase of Ag-NPs-induced plasmon and the logarithm of the cysteine concentration was obtained within a range of 20−400 nM (lg) with a correlation coefficient R of 0.997 (Figure 6B). The linear regression equation is $\Delta Abs = 0.387 \lg C_{Cys} - 0.248$, giving rise to a detection limit of 8.5 nM (3σ/s, $n = 9$) and a precision of 3.3% RSD (100 nM, $n = 11$). Moreover, the calibration range can be regulated by simply varying the concentration of Ag^+. Figure 6C showed that ultra sensitive assay of biothiols is feasible by using lower concentration of Ag^+; that is, when using 0.1 mM Ag^+, a linear range close to the above lower detection limit, i.e., 2.5−30 nM, is obtained (Figure 6D), with a linear regression equation of $\Delta Abs = 0.00664 C_{Cys} + 0.229$. This gives rise to a detection limit of 1.5 nM (3σ/s, $n = 11$) and a precision of 3.1% RSD at 20 nM. Our experimental results have indicated that the present optosensing system could be similarly applied for an ultrasensitive assay of homocysteine (Hcy) and glutathione (GSH) as illustrated in Figure 7. The linear calibration curves were obtained within 5−40 nM and 2.5−30 nM for Hcy and GSH, respectively, achieving detection limits

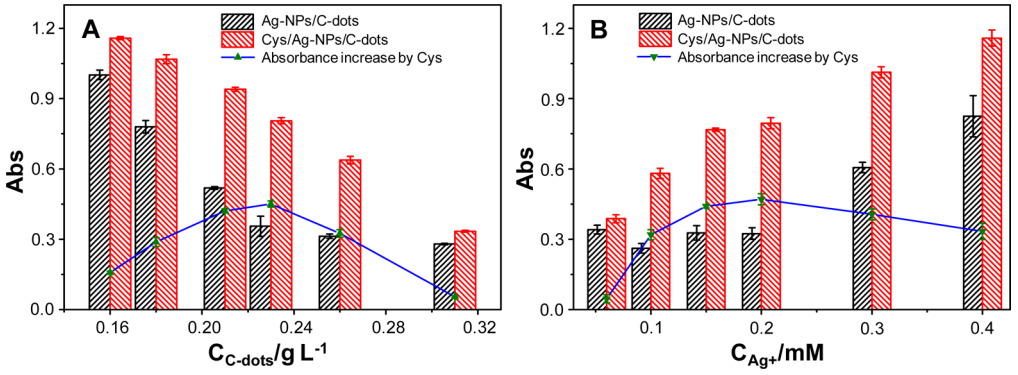

Figure 5. (A) C-dots (0.16−0.31 g L^{-1}) concentration-dependent absorbance at 430 nm for the derived Ag-NPs in the absence and presence of Cys (100 nM) along with the variation of net increase of absorbance with C-dots concentration, 0.2 mM $AgNO_3$, 0.01 M NaOH at 50 °C for 5 min; (B) $AgNO_3$ (0.06−0.4 mM) concentration-dependent absorbance at 430 nm for the derived Ag-NPs in the absence and presence of Cys (100 nM) along with the variation of net increase of absorbance as a function of $AgNO_3$ concentration, 0.23 g L^{-1} C-dots, 0.01 M NaOH at 50 °C for 5 min.

dx.doi.org/10.1021/ac500601k | Anal. Chem. 2014, 86, 5002−5008

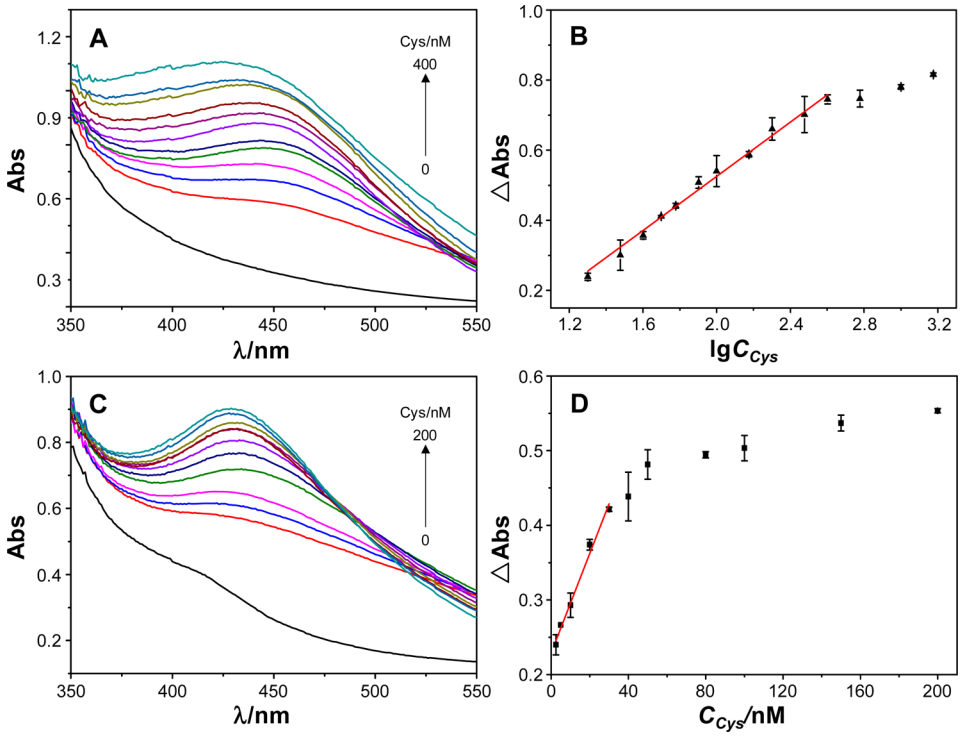

Figure 6. (A) UV−vis spectra of the Cys/Ag-NPs/C-dots composite with different concentrations of Cys, Ag^+ (0.2 mM), C-dots (0.23 g L^{-1}), and NaOH (0.01 M), 50 °C for 5 min. (B) The linear calibration graph between net increase of absorbance at 430 nm and Cys concentration (logarithm). (C) UV−vis spectra of the Cys/Ag-NPs/C-dots composite with different concentrations of Cys, Ag^+ (0.1 mM), C-dots (0.21 g L^{-1}), and NaOH (0.05 M), 70 °C for 5 min. (D) The linear calibration graph between net increase of absorbance at 430 nm and Cys concentration.

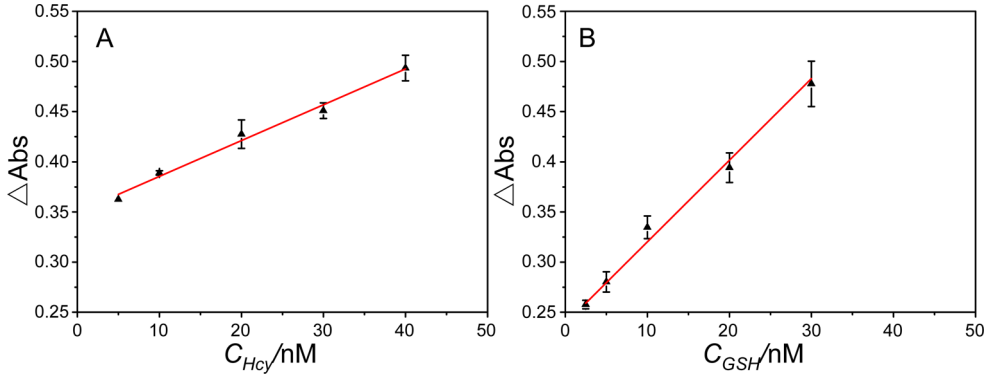

Figure 7. Linear calibration graph between net absorbance increase at 430 nm and the concentrations of Hcy (A) and GSH (B). C-dots (0.21 g L^{-1}), Ag^+ (0.1 mM), NaOH (0.05 M), 70 °C for 5 min.

of 2.6 and 1.2 nM and precisions of 3.1% and 2.4% at 20 nM, respectively. It is obvious that the system provides comparable sensitivity to the three biothiols. Hcy has stronger reducing capability than Cys and GSH; thus, the release of Ag^+ from Cys-Ag^+ and GSH-Ag^+ complexes might be easier than that for the Hcy-Ag^+ complex.[17] When compared to the other colorimetric assay approaches for biothiols, the present system provides a more sensitive label-free procedure (Table 1).

Specificity of Biothiols on the Growth of Ag-NPs. In order to demonstrate the specificity for thiol-containing compounds by using the present sensing system, we have investigated the response of the system to 19 other essential amino acids as illustrated in Figure 8. It is obvious that 20 nM Cys resulted in a significant enhancement on the growth of Ag-NPs, whereas no absorbance changes were observed for the other amino acids even at a much higher concentration of 3000 nM. To further evaluate the selectivity of the system for the assay of biothiols, we investigated the effect of major metal cations and other molecules in biological fluids, e.g., Ca^{2+} (50 μM), Mg^{2+} (50 μM), HSA (0.76 μM), glucose (50 μM), and ascorbic acid (50 μM). As shown in Figure 8, the enhancement of the absorbance due to the addition of these foreign species was virtually well controlled below ±5%. This indicated that the present sensing system offers favorable sensitivity and selectivity for the assay of biothiols in the presence of essential biological species or molecules in real biological samples.

Specific Assay of Cysteine in Human Plasma Samples. The applicability and reliability of the present sensing system for the assay of cysteine was evaluated by analyzing human plasma samples. The analytical results are given in Table 2. The addition of serum sample into the C-dots/Ag^+ solution led to the increase of absorbance at 430 nm, while no obvious change

dx.doi.org/10.1021/ac500601k | Anal. Chem. 2014, 86, 5002−5008

Table 1. Comparison of the Sensitivity for the Present Sensing System with Other Colorimetric Procedures for Biothiols

label	species	detection limit, nM
2,2′-azinobis(3-ethylbenzthiazoline-6-sulfonate)[21]	Cys	40
2,2′-azinobis(3-ethylbenzthiazoline-6-sulfonate)[22]	Cys	50
	GSH	40
gold nanoparticles[24]	Cys	100
gold nanorods[26]	Cys	10
gold nanoparticles[27]	Cys	200
	Hcy	200
gold nanoparticles[61]	Cys	166
label free (this method)	Cys	2.5
	Hcy	5
	GSH	2.5

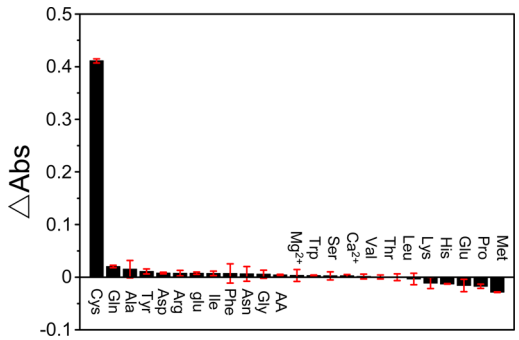

Figure 8. Increase of absorbance at 430 nm of Ag-NPs in the presence of various amino acids, metal cations, and biological molecules. The concentrations of Cys, amino acids, metal cations, and biological molecules were 20 nM, 3 μM, 50 μM, and 0.76 μM, respectively.

Table 2. Assay Results of Cysteine in Human Plasma Samples

sample	found[a]/μM	spiked/μM	recovered[a]/μM	recovery/%
serum 1	156.8 ± 3.3	100	251.8 ± 16.1	95
serum 2	124.4 ± 17.0	100	232.7 ± 2.9	108
serum 3	204.0 ± 5.9	100	298.4 ± 3.9	94

[a] n = 3, means $\pm t{\cdot}s/\sqrt{n}$, f = 95%, t = 3.18.

was observed in the sample pretreated with the thiol-blocking reagent NEM, which demonstrated that the increase of absorbance of the sensing system was actually attributed to the biothiols in the serum sample. Afterward, spiking recovery was performed by adding a certain amount of cysteine into the plasma samples followed by assaying with the present procedure. Recoveries within 94−108% were achieved, indicating the accuracy and reliability of the present method and its suitability in routine analysis.

CONCLUSIONS

In contrast to the conventional principles for quenching the fluorescence of C-dots with analytes, the present study constructed an ultra sensitive and selective Ag-NPs plasmon absorption-based colorimetric optosensor for the assay of biothiols. The procedure is developed by taking advantage of the catalytic reducing capability of C-dots and its regulation on the growth of Ag-NPs in the presence of biothiols through progressive release of free Ag^+ from the preformed Ag^+-biothiol complex. A colorimetric assay procedure based on Ag-NPs plasmon absorption is developed for fast detection of biothiols, which is particularly suitable for an ultratrace amount of biothiols. The performance of the procedure reported herein has been demonstrated for the assay of biothiols in human serum samples. This study provides an approach for the development of new assay methodologies for molecules of biological significance.

ASSOCIATED CONTENT

Supporting Information

UV−vis absorption spectra. This material is available free of charge via the Internet at http://pubs.acs.org/.

AUTHOR INFORMATION

Corresponding Authors

*E-mail: chenxuwei@mail.neu.edu.cn. Tel: +86-24-83688944. Fax: +86-24-83676698.

*E-mail: jianhuajrz@mail.neu.edu.cn. Tel: +86-24-83688944. Fax: +86-24-83676698.

Notes

The authors declare no competing financial interest.

ACKNOWLEDGMENTS

This work is financially supported by the Natural Science Foundation of China (21275027, 21235001, 21375013), the Program of New Century Excellent Talents in University (NCET-11-0071), and Fundamental Research Funds for the Central Universities (N110805001, N120405004, and N130105002).

REFERENCES

(1) Basford, R. E.; Huennekens, F. M. *J. Am. Chem. Soc.* **1955**, *77*, 3873−3877.
(2) Zhang, S.; Ong, C.-N.; Shen, H.-M. *Cancer Lett.* **2004**, *208*, 143−153.
(3) Shahrokhian, S. *Anal. Chem.* **2001**, *73*, 5972−5978.
(4) Wang, X. F.; Cynader, M. S. *J. Neurosci.* **2001**, *21*, 3322−3331.
(5) Sehadri, S.; Beiser, A.; Selhub, J.; Jacques, P. F.; Rosenberg, I.; D'agostino, R. B.; Wilson, P. W. F.; Wolf, P. A. *N. Engl. J. Med.* **2002**, *346*, 476−483.
(6) Refsum, H.; Ueland, P. M.; Nygard, O.; Vollset, S. E. *Annu. Rev. Med.* **1998**, *49*, 31−62.
(7) Kleinman, W. A.; Richie, J. P. *Biochem. Pharmacol.* **2000**, *60*, 19−29.
(8) Staal, F. J. T.; Ela, S. W.; Roederer, M.; Anderson, M. T.; Herzenberg, L. A.; Herzenberg, L. A. *Lancet* **1992**, *339*, 909−912.
(9) Chen, X.; Zhou, Y.; Peng, X.; Yoon, J. *Chem. Soc. Rev.* **2010**, *39*, 2120−2135.
(10) Jung, H. S.; Chen, X.; Kim, J. S.; Yoon, J. *Chem. Soc. Rev.* **2013**, *42*, 6019−6031.
(11) Mei, J.; Wang, Y.; Tong, J.; Wang, J.; Qin, A.; Sun, J. Z.; Tang, B. Z. *Chem.—Eur. J.* **2013**, *19*, 613−620.
(12) Wang, W.; Rusin, O.; Xu, X.; Kim, K. K.; Escobedo, J. O.; Fakayode, S. O.; Fletcher, K. A.; Lowry, M.; Schowalter, C. M.; Lawrence, C. M.; Fronczek, F. R.; Warner, I. M.; Strongin, R. M. *J. Am. Chem. Soc.* **2005**, *127*, 15949−15958.
(13) Xu, K.; Chen, H.; Wang, H.; Tian, J.; Li, J.; Li, Q.; Li, N.; Tang, B. *Biosens. Bioelectron.* **2011**, *26*, 4632−4636.
(14) Tang, B.; Xing, Y.; Li, P.; Zhang, N.; Yu, F.; Yang, G. *J. Am. Chem. Soc.* **2007**, *129*, 11666−11667.
(15) Zhang, M.; Yu, M.; Li, F.; Zhu, M.; Li, M.; Gao, Y.; Li, L.; Liu, Z.; Zhang, J.; Zhang, D.; Yi, T.; Huang, C. *J. Am. Chem. Soc.* **2007**, *129*, 10322−10323.
(16) Zhang, Y.; Li, Y.; Yan, X.-P. *Anal. Chem.* **2009**, *81*, 5001−5007.

(17) Sun, S.-K.; Wang, H.-F.; Yan, X.-P. *Chem. Commun.* **2011**, *47*, 3817−3819.
(18) Stobiecka, M.; Molinero, A. A.; Chałupa, A.; Hepel, M. *Anal. Chem.* **2012**, *84*, 4970−4978.
(19) Stobiecka, M.; Hepel, M. *Sens. Actuators, B: Chem.* **2010**, *149*, 373−380.
(20) Stobiecka, M.; Deeb, J.; Hepel, M. *Biophys. Chem.* **2010**, *146*, 98−107.
(21) Li, T.; Shi, L.; Wang, E.; Dong, S. *Chem.—Eur. J.* **2009**, *15*, 3347−3350.
(22) Zhou, X.-H.; Kong, D.-M.; Shen, H.-X. *Anal. Chem.* **2010**, *82*, 789−793.
(23) Xu, H.; Hepel, M. *Anal. Chem.* **2011**, *83*, 813−819.
(24) Lee, J.-S.; Ulmann, P. A.; Han, M. S.; Mirkin, C. A. *Nano Lett.* **2008**, *8*, 529−533.
(25) Sudeep, P. K.; Joseph, S. T. S.; Thomas, K. G. *J. Am. Chem. Soc.* **2005**, *127*, 6516−6517.
(26) Huang, H.; Liu, X.; Hu, T.; Chu, P. K. *Biosens. Bioelectron.* **2010**, *25*, 2078−2083.
(27) Xiao, Q.; Shang, F.; Xu, X.; Li, Q.; Lu, C.; Lin, J.-M. *Biosens. Bioelectron.* **2011**, *30*, 211−215.
(28) Lu, C.; Zu, Y. *Chem. Commun.* **2007**, 3871−3873.
(29) Baker, S. N.; Baker, G. A. *Angew. Chem., Int. Ed.* **2010**, *49*, 6726−6744.
(30) Sun, Y.-P.; Zhou, B.; Lin, Y.; Wang, W.; Fernando, K. A. S.; Pathak, P.; Meziani, M. J.; Harruff, B. A.; Wang, X.; Wang, H.; Luo, P. G.; Yang, H.; Kose, M. E.; Chen, B.; Veca, L. M.; Xie, S.-Y. *J. Am. Chem. Soc.* **2006**, *128*, 7756−7757.
(31) Zheng, L.; Chi, Y.; Dong, Y.; Lin, J.; Wang, B. *J. Am. Chem. Soc.* **2009**, *131*, 4564−4565.
(32) Liu, R.; Wu, D.; Liu, S.; Koynov, K.; Knoll, W.; Li, Q. *Angew. Chem., Int. Ed.* **2009**, *48*, 4598−4601.
(33) Pan, D.; Zhang, J.; Li, Z.; Wu, C.; Yan, X.; Wu, M. *Chem. Commun.* **2010**, *46*, 3681−3683.
(34) Zhu, C.; Zhai, J.; Dong, S. *Chem. Commun.* **2012**, *48*, 9367−9369.
(35) Yang, S.-T.; Cao, L.; Luo, P. G.; Lu, F.; Wang, X.; Wang, H.; Meziani, M. J.; Liu, Y.; Qi, G.; Sun, Y.-P. *J. Am. Chem. Soc.* **2009**, *131*, 11308−11309.
(36) Zhu, S.; Meng, Q.; Wang, L.; Zhang, J.; Song, Y.; Jin, H.; Zhang, K.; Sun, H.; Wang, H.; Yang, B. *Angew. Chem., Int. Ed.* **2013**, *52*, 3953−3957.
(37) Zhou, L.; Li, Z.; Liu, Z.; Ren, J.; Qu, X. *Langmuir* **2013**, *29*, 6396−6403.
(38) Li, H.; He, X.; Kang, Z.; Huang, H.; Liu, Y.; Liu, J.; Lian, S.; Tsang, C. H. A.; Yang, X.; Lee, S.-T. *Angew. Chem., Int. Ed.* **2010**, *49*, 4430−4434.
(39) Guo, X.; Wang, C.-F.; Yu, Z.-Y.; Chen, L.; Chen, S. *Chem. Commun.* **2012**, *48*, 2692−2694.
(40) Huang, X.; Zhang, F.; Zhu, L.; Choi, K. Y.; Guo, N.; Guo, J.; Tackett, K.; Anilkumar, P.; Liu, G.; Quan, Q.; Choi, H. S.; Niu, G.; Sun, Y.-P.; Lee, S.; Chen, X. *ACS Nano* **2013**, *7*, 5684−5693.
(41) Shi, W.; Li, X.; Ma, H. *Angew. Chem., Int. Ed.* **2012**, *51*, 6432−6435.
(42) Dong, Y.; Wang, R.; Li, H.; Shao, J.; Chi, Y.; Lin, X.; Chen, G. *Carbon* **2012**, *50*, 2810−2815.
(43) Zhou, L.; Lin, Y.; Huang, Z.; Ren, J.; Qu, X. *Chem. Commun.* **2012**, *48*, 1147−1149.
(44) Qu, Q.; Zhu, A.; Shao, X.; Shi, G.; Tian, Y. *Chem. Commun.* **2012**, *48*, 5473−5475.
(45) Lu, W.; Qin, X.; Liu, S.; Chang, G.; Zhang, Y.; Luo, Y.; Asiri, A. M.; Al-Youbi, A. O.; Sun, X. *Anal. Chem.* **2012**, *84*, 5351−5357.
(46) Liu, S.; Tian, J.; Wang, L.; Zhang, Y.; Qin, X.; Luo, Y.; Asiri, A. M.; Al-Youbi, A. O.; Sun, X. *Adv. Mater.* **2012**, *24*, 2037−2041.
(47) Wang, X.; Cao, L.; Lu, F.; Meziani, M. J.; Li, H.; Qi, G.; Zhou, B.; Harruff, B. A.; Kermarrec, F.; Sun, Y.-P. *Chem. Commun.* **2009**, 3774−3776.
(48) Wang, X.; Long, Y.; Wang, Q.; Zhang, H.; Huang, X.; Zhu, R.; Teng, P.; Liang, L.; Zheng, H. *Carbon* **2013**, *64*, 499−506.
(49) Dey, D.; Bhattacharya, T.; Majumdar, B.; Mandani, S.; Sharma, B.; Sarma, T. K. *Dalton Trans.* **2013**, *42*, 13821−13825.
(50) Luo, P.; Li, C.; Shi, G. *Phys. Chem. Chem. Phys.* **2012**, *14*, 7360−7366.
(51) Zhang, Y.; Xing, C.; Jiang, D.; Chen, M. *CrystEngComm* **2013**, *15*, 6305−6310.
(52) Shen, L.; Chen, M.; Hu, L.; Chen, X.; Wang, J. *Langmuir* **2013**, *29*, 16135−16140.
(53) Yang, Y.; Cui, J.; Zheng, M.; Hu, C.; Tan, S.; Xiao, Y.; Yang, Q.; Liu, Y. *Chem. Commun.* **2012**, *48*, 380−382.
(54) Shen, J.-S.; Li, D.-H.; Zhang, M.-B.; Zhou, J.; Zhang, H.; Jiang, Y.-B. *Langmuir* **2011**, *27*, 481−486.
(55) Xia, Y.; Xiong, Y.; Lim, B.; Skrabalak, S. E. *Angew. Chem., Int. Ed.* **2009**, *48*, 60−103.
(56) Lamer, V. K.; Dinegar, R. H. *J. Am. Chem. Soc.* **1950**, *72*, 4847−4854.
(57) Liu, H.; Ye, Y.; Chen, J.; Lin, D.; Jiang, Z.; Liu, Z.; Sun, B.; Yang, L.; Liu, J. *Chem.—Eur. J.* **2012**, *18*, 8037−8041.
(58) Nan, J.; Yan, X.-P. *Chem.—Eur. J.* **2010**, *16*, 423−427.
(59) Mandal, S.; Gole, A.; Lala, N.; Gonnade, R.; Ganvir, V.; Sastry, M. *Langmuir* **2001**, *17*, 6262−6268.
(60) Mafune, F.; Kohno, J.-Y.; Takeda, Y.; Kondow, T. *J. Phys. Chem. B* **2000**, *104*, 9111−9117.
(61) Qian, Q.; Deng, J.; Wang, D.; Yang, L.; Yu, P.; Mao, L. *Anal. Chem.* **2012**, *84*, 9579−9584.